Delivery of bioactive molecules to the mitochondrial genome using a membrane-fusing, liposome-based carrier, DF-MITO-Porter

Yuma Yamada[a] and Hideyoshi Harashima[a]*

[a] Laboratory for molecular design of pharmaceutics, Faculty of Pharmaceutical Sciences, Hokkaido University, Kita-12, Nishi-6, Kita-ku, Sapporo 060-0812, Japan

*Corresponding author: Laboratory for molecular design of pharmaceutics, Faculty of Pharmaceutical Sciences, Hokkaido University, Kita-12, Nishi-6, Kita-ku, Sapporo 060-0812, Japan

Tel: +81-11-706-3919 Fax: +81-11-706-4879

E-mail: harasima@pharm.hokudai.ac.jp

Abstract Mitochondrial dysfunction has been implicated in a variety of human diseases. It is now well accepted that mutations and defects in the mitochondrial genome form the basis of these diseases. Therefore, mitochondrial gene therapy and diagnosis would be expected to have great medical benefits. To achieve such ~~an innovative~~ a strategy, it will be necessary to deliver therapeutic agents into mitochondria in living cells. We report here on ~~a novel~~ an approach to accomplish this via the use of a Dual Function (DF)-MITO-Porter, aimed at the mitochondrial genome, so-called mitochondrial DNA (mtDNA). The DF-MITO-Porter, ~~an innovative~~ a nano carrier for mitochondrial delivery, has the ability to penetrate the endosomal and mitochondrial membranes via step-wise membrane fusion. We first constructed a DF-MITO-Porter encapsulating DNase I protein as a bioactive cargo. It was expected that mtDNA would be digested, when the DNase I was delivered to the mitochondria. We observed the intracellular trafficking of the carriers, and then measured mitochondrial activity and mtDNA-levels after the delivery of DNase I by the DF-MITO-Porter. The findings confirm that the DF-MITO-Porter effectively delivered the DNase I into the mitochondria, and provides a demonstration of its potential use in therapies that are selective for the mitochondrial genome.

Key words: Mitochondria; Mitochondrial drug delivery; Mitochondrial gene therapy; MITO-Porter; Membrane fusion; mitochondrial DNA (mtDNA).

1. Introduction

Mutations and defects in mitochondrial DNA (mtDNA) have been associated with various mitochondrial dysfunctions, which form the basis of a variety of human disorders including neurodegenerative and neuromuscular diseases [1-7]. For example, a mutation in mtDNA in the region that encodes for tRNA causes mitochondrial myopathy, encephalopathy, lactic acidosis and stroke-like episodes (MELAS) [8] and myoclonic epilepsy with ragged-red fibers (MERRF) [9]. In addition, deletions in mtDNA have been discovered in the majority of cases of chronic progressive external ophthalmoplegia (CPEO) and cases of the Kearns-Sayre syndrome (KSS) [10]. Therefore, mitochondrial gene therapy and diagnosis promises to be useful and productive in the treatment of many patients suffering from these intractable diseases.

To achieve such ~~an innovative~~ a strategy to target mitochondrial genome, it will be ultimately necessary to develop an optimal drug delivery system, which will likely be achieved through innovation associated with the nanotechnology of intracellular trafficking. In addition, for the strategy to be successful, it will be necessary to deliver therapeutic/diagnostic agents into the innermost mitochondrial space, the mitochondrial matrix, where the mtDNA pool is located. A number of systems for delivering cargoes to mitochondria have been reported to date [11-13]. However, reports of mitochondrial genome targeting by means of an artificial gene vector are limited, although endogenous

mitochondrial importing signal RNA can deliver exogenous RNA to mitochondria in mammalian cells [14, 15]. Weissig and coworkers reported on the development of DQAsomes, which are mitochondriotropic and cationic vesicles designed for mitochondrial-targeted DNA delivery [16, 17]. They showed that DQAsomes specifically release pDNA proximal to mitochondria in living cells [17, 18], although the delivery of cargoes into the interior of mitochondria has not been validated.

In previous studies, we proposed the use of a MITO-Porter, which is a liposome-based nano carrier that delivers cargos to mitochondria via membrane fusion [19]. Using the green fluorescent protein as a model macromolecule and analysis by confocal laser scanning microscopy (CLSM), we were able to confirm mitochondrial macromolecule delivery of a macromolecule by the MITO-Porter. Moreover, we verified that the MITO-Porter could deliver cargos into the mitochondrial matrix, which contains the mtDNA pool [20]. We utilized propidium iodide, PI, an impermeable red fluorescence-dye for nucleic acids, as a probe to detect mtDNA. When the MITO-Porter was added to living cells, strong red-signals were detected within mitochondria, suggesting that the carrier had the ability to deliver PI to the mitochondrial matrix in living cells.

In this study, we report on ~~a novel~~ an approach for the mitochondrial delivery of

bioactive molecules using a Dual Function (DF)-MITO-Porter, aimed at mtDNA. The DF-MITO-Porter, which possesses mitochondria-fusogenic inner and endosome-fusogenic outer envelopes, has the ability to pass through endosomal and mitochondrial membranes via step-wise membrane fusion (Figure 1) [21]. Octaarginine (R8) functions as a cell-uptake device [22, 23] in the outer envelope and as a mitochondrial targeting device [12, 24, 25] in the inner envelope. In this experiment, we attempted to deliver DNase I protein to mitochondria in living cells. It was expected that mtDNA would be digested, resulting in a reduction in mitochondrial activity, when the mitochondrial delivery of DNase I progressed, as shown in Figure 1.

We first constructed a DF-MITO-Porter encapsulating DNase I and observed the intracellular trafficking of the DNase I delivered by DF-MITO-Porter using CLSM. We then measured the activity of mitochondrial dehydrogenase to confirm that the digestion of mtDNA by DNase I influenced mitochondrial activity. Moreover, we quantified the levels of mtDNA and nuclear DNA after the mitochondrial delivery of DNase I to demonstrate its potential use in therapies that are aimed selectively at mtDNA.

2. **Materials and methods**

2.1. Materials

1, 2-Dioleoyl-sn-glycero-3-phosphatidyl ethanolamine (DOPE) was purchased from Avanti Polar lipids (Alabaster, AL, USA). Egg yolk phosphatidyl choline (EPC) was obtained from Nippon Oil and Fats Co. (Tokyo, Japan). Cholesteryl hemisuccinate (5-cholesten-3-ol 3-hemisuccinate; CHEMS), phosphatidic acid (PA) and sphingomyelin (SM) were purchased from Sigma (St. Louis, MO, USA). Stearyl octaarginine (STR-R8) [26] was obtained from KURABO INDUSTRIES LTD (Osaka, Japan). DNase I protein (from bovine pancreas, Grade II) was purchased from Roche Diagnostics GmbH (Mannheim Germany). Alexa Fluor-488 labeled DNase I was prepared using an Alexa Fluor 488 Protein Labeling Kit (Invitrogen Corporation, Carlsbad, CA, USA) according to the supplier's instructions. HeLa human cervix carcinoma cells were obtained from the RIKEN Cell Bank (Tsukuba, Japan). Dulbecco's modified Eagle medium (DMEM), fetal bovine serum (FBS) and Mitofluor Red 589 were purchased from Invitrogen Corp. All other chemicals used were commercially available reagent-grade products.

2.2. Construction of DF-MITO-Porter encapsulating DNase I

The DNase I-encapsulated Dual Function (DF)-MITO-Porter was constructed by the multi-layering method, as previously reported (see Figure S1 in supplementary data for details) [21]. DNase I protein was gently mixed with the STR-R8, as complex-inducer, in 100 μL of 10 mM HEPES buffer (pH 7.4), followed by incubation for 15 min at 25ºC to form complexed protein particles. Particles of the DNase I/STR-R8 were formed using 50 μg of DNase I at a complex-inducer/protein (C/P) molar ratio of 10. For the inner and outer envelopes, various small unilamellar vesicles (SUVs) were prepared as shown in supplementary data. The lipid composition and properties of the SUVs are summarized in Table S1. The suspended negatively charged SUVs and complexed protein particles were mixed at a ratio of 3 : 1 (v/v) to coat the complexed protein particles with a double-lipid envelope to produce a di-lamellar structured nanoparticle (D-SNP). These SUVs were composed of mitochondria-fusogenic lipid [DOPE/PA = 9 : 2, DOPE/SM/CHEMS = 9 : 2 : 1 (molar ratio)] or non-fusogenic lipid [EPC/CHEMS = 9 : 2 (molar ratio)]. An STR-R8 solution (10 mol% of total lipid) was added to the suspension of D-SNPs to reverse the surface charge. This suspension was then mixed with endosome-fusogenic SUV [DOPE/PA = 7 : 2 (molar ratio)] at a ratio of 1 : 2 (v/v) to generate particles with a double endosome-fusogenic envelope, hereafter referred to as a tetra-lamellar structured

nanoparticle (T-SNP). The STR-R8 solution (10 mol% of endosome-fusogenic lipid) was added to the suspension of T-SNP to modify the outer envelope with R8. We refer to the R8 modified T-SNP with a mitochondria-fusogenic inner envelope that contains PA and SM as the DF-MITO-Porter (PA) and the DF-MITO-Porter (SM), respectively. Particle diameters were measured using a quasi-elastic light scattering method, and ζ potentials were determined electrophoretically using laser doppler velocimetry (Zetasizer Nano ZS; Malvern Instruments, Herrenberg, Germany).

2.3. Intracellular observation of DNase I encapsulated in DF-MITO-Porter using confocal laser scanning microscopy

HeLa cells (4 x 10^4 cells) were cultured in 35 mm dishes (BD Falcon, NJ) with DMEM, which contained 10% FBS, under an atmosphere of 5% CO_2 / air at 37ºC for 24 ± 3 hr. The carriers encapsulating DNase I protein labeled with 5 mol% of Alexa488 were added to the HeLa cells (final concentration of DNase I protein, 2 μg/mL). The cells were then incubated in phenol red-free medium in the absence of serum under an atmosphere of 5% CO_2/air at 37ºC. After a 1-hr incubation, the medium was replaced with fresh phenol red-free medium containing serum, and the cells were incubated in the absence of the carriers for 2 hr. The cells were observed by confocal laser scanning

microscopy (CLSM) after staining the mitochondria.

Thirty minutes before acquiring the fluorescence images, the medium was replaced with fresh medium containing Mitofluor Red 589 (final concentration, 100 nM) and the cells were incubated in this solution. After the incubation, the cells were washed with the phenol red-free medium containing serum, and then observed by CLSM (FV10i-LIV; Olympus Corporation, Tokyo, Japan). The cells were excited with a 473 nm light and a 559 nm light from a LD laser. Images were obtained using a FV10i-LIV equipped with a water-immersion objective lens (UPlanSApo 60x/NA = 1.2) and a dichroic mirror (DM405/473/559/635). The two fluorescence detection channels (Ch) were set to the following filters: Ch1: 490/100 (green color) for Alexa 488 and Ch2: 570/100 (red color) for Mitofluor Red 589.

2.4. Evaluation of mitochondrial activity

HeLa cells (1 x 10^4 cells/well) were incubated in a 24 well plate (Corning, NY, USA) with DMEM containing 10% FBS, under 5% CO_2 / air at 37°C for 24 hr. Sample-suspensions in 0.25 mL of serum-free DMEM were added to the cells after washing them with phosphate-buffer saline (PBS (-)), followed by incubation under 5% CO_2 at 37°C for 3 hr. After replacing the medium with fresh DMEM containing 10%

serum, the cells were incubated for a further 21 hr. The cells were then washed with PBS (-), and mitochondrial dehydrogenase activity was measured using a Cell Proliferation Assay System with a Tetra Color ONE (SEIKAGAKU BIOBUSINESS CORPORATION, Tokyo, Japan) by means of a Benchmark plus microplate reader (Bio-Rad Laboratories, Inc., CA, USA). The assay is based on the cleavage of the tetrazolium salt 2-(2-Methoxy-4-nitrophenyl)-3-(4-nitrophenyl)-5-(2,4-disulfophenyl)-2H-tetrazolium, monosodiumsalt (WST)-8 by mitochondrial dehydrogenase in viable cells to create a formazan dye. Mitochondrial activity was calculated as follows;

$$\text{Mitochondrial activity (\%)} = A_S / A_U \times 100$$

where A_S, A_U represent the mitochondrial dehydrogenase activity when cells were treated and untreated with samples, respectively.

2.5. Evaluation for the levels of mtDNA and nuclear DNA after the mitochondrial delivery of DNase I.

HeLa cells (2×10^5 cells/well) were seeded on a 6-well plate (Corning) with DMEM containing 10% FBS, under 5% CO_2 / air at 37°C for 24 hr. Sample-suspensions containing 6 μg of DNase I in 1 mL of serum-free DMEM were

added to the cells after washing them with PBS (-), followed by incubation under 5% CO_2 at 37°C for 3 hr. After the addition of fresh DMEM containing 10% serum, the cells were incubated for a further 21 hr. The cells were then washed with PBS (-), trypsinized, suspended in DMEM with serum, precipitated by centrifugation (1,800*g*, 4ºC, 3 min). The pellets were washed with PBS (-) and precipitated by centrifugation (1,800*g*, 4ºC, 3 min). To evaluate the levels of mtDNA and nuclear DNA, total cellular DNA was isolated from cell lysates and purified by means of a GenElute Mammalian Genome DNA Miniprep kit (Sigma–Aldrich, St. Louis, MO, USA) and subjected to the PCR.

The PCR reaction mixture contained, in a total volume of 25 μL, 10 mM of Tris-HCl (pH 8.3), 1.5 mM of $MgCl_2$, 50 mM of KCl, 200 μM of each one of the deoxynucleoside triphosphates, 0.5 μM of primers ND6 (+) and ND6 (-) for mtDNA detection or primers β-Actin (+) and β-Actin (-) for nuclear DNA (Table S2), and 10 ng of DNA obtained from HeLa cell lysates. After the addition of 0.625 U of Taq DNA polymerase (Finnzymes PCR Reagents; Thermo Fisher Scientific, Waltham, MA, USA), the reaction mixture was first incubated at 94ºC for 2 min, then subjected to 30 cycles of 30 sec at 94^{o}C, 30 sec at 55^{o}C and 45 sec at 72^{o}C, and finally to 10 min at 72^{o}C. Each 5μL of PCR products were subjected to electrophoresis in 2% agarose gel in TAE (40

mM Tris-HCl, 40 mM acetic acid, 1 mM EDTA, pH 8.0) at 100 V for 30 min. The DNA bands were visualized by UV after ethidium bromide staining.

The intensity of the PCR product band was determined using the Image J v.1.40 software (National Institutes of Health, USA). Relative amounts of DNA were calculated as follows:

Relative amount of DNA = (intensity of the PCR product band in samples / intensity of the PCR product in non-treatment).

3. Results

3.1. Construction of DF-MITO-Porter encapsulating DNase I

The DF-MITO-Porter encapsulating DNase I was constructed as described in our previous reports (see Figure S1 in supplementary data for details) [21]. Complexed DNase I particles were first prepared with STR-R8, and were then coated with a mitochondria-fusogenic envelope. Finally, the envelopes were further coated with an endosome-fusogenic envelope. The size and ζ-potential of the DF-MITO-Porter and control carrier are summarized in Table S3. Particle diameters were around 150 nm and the ζ-potentials were around + 30 mV. The outer envelope of all carriers had a endosome-fusogenic composition [27]. For the DF-MITO-Porter, the inner envelope had a mitochondria-fusogenic composition [19], while a non-mitochondrial fusogenic composition[19] was used in the control inner envelope. We also prepared a conventional MITO-Porter for purposes of checking the multi-layered structure (Table S3).

3.2. Intracellular observation of DNase I encapsulated in DF-MITO-Porter using confocal laser scanning microscopy

We performed the intracellular observation of DNase I encapsulated in the

DF-MITO-Porter and the conventional MITO-Porter using CLSM (Fig. 2). We incubated the carrier encapsulating Alexa488, a fluorescent dye, labeled DNase I protein, with HeLa cells, and then stained the mitochondria with Mitofluor Red 589. In the case of the DF-MITO-Porter, numerous yellow clusters were observed (Fig. 2A), indicating that the green dots, Alexa488 in DNase I proteins were co-localized with red stained mitochondria and observed as a yellow signals. When the conventional MITO-Porter without endosome fusogenic envelopes was used, yellow dots were observed in the cells, but most of the DNase I were located outside mitochondria, as evidenced by the location of the green dots (Fig. 2B). These findings suggest that a multi-layered structure with different lipid compositions can be very useful for mitochondrial delivery in living cells.

3.3. Mitochondrial delivery of DNase I using the DF-MITO-Porter and evaluation of the mitochondrial activity

Mitochondrial activity was evaluated by measuring the activity of mitochondrial dehydrogenase after the delivery of DNase I (0.5 μg) by the DF-MITO-Porter. In this experiment, mitochondrial activity would be predicted to be inversely proportional to the efficiency of the mitochondrial delivery of DNase I. The use of the DF-MITO-Porter

resulted in a significant decrease in mitochondrial activity, whereas carriers with a low mitochondrial fusion activity had only a negligible effect on mitochondrial activity (Fig. 3A). This result suggests that the DF-MITO-Porter is able to deliver extracellular bioactive molecules into the mitochondria and that the delivered molecules are functional for the mitochondrial genome.

We also evaluated mitochondrial activity after the mitochondrial delivery of DNase I protein (6.25 μg) using a conventional MITO-Porter without endosome fusogenic outer envelopes (Fig. 3B). The envelope of the conventional MITO-Porters had a mitochondria-fusogenic composition [DOPE/SM/CHEMS/STR-R8 (9:2:1:1, molar ratio) or DOPE/PA/STR-R8 (9:2:1, molar ratio)]. In the case where the conventional MITO-Porter included the PA (MITO-Porter (PA)), mitochondrial activity was significantly decreased, whereas the conventional MITO-Porter including the SM (MITO-Porter (SM)) had only a negligible effect on mitochondrial activity. These results indicate that the conventional MITO-Porter (PA) had a higher mitochondrial targeting activity than that of the conventional MITO-Porter (SM), although the mitochondrial fusogenic activities of the carriers were similar, as we previously reported [19].

Moreover, we evaluated the mitochondrial activities between DF-MITO-Porter

and the conventional MITO-Porter. Figure 4 provides information on the applied dose of DNase I (x-axis) and mitochondrial activity (y-axis). We calculated the effective dose 50 (ED_{50}) for each carrier, and the results indicated that the DF-MITO-Porter (ED_{50}=0.33 μg) was 15-fold more efficient than the conventional MITO-Porter (ED_{50}=5.4 μg) in mitochondrial delivery.

3.4. Evaluation for the levels of mtDNA and nuclear DNA after the mitochondrial delivery of DNase I using the DF-MITO-Porter

To verify that the decrease of mitochondrial activity was the result of the digestion of mtDNA as the result of the mitochondrial delivery of DNase I, we evaluated cellular mtDNA-levels using PCR analysis (Fig. 5). After the delivery of DNase I, the cellular DNAs were collected and subjected to the PCR using the primer sets shown in Table S2. PCR assays for the detection of the ND6 and β-Actin genes were performed in order to detect both mtDNA and nuclear DNA. The PCR products were then detected by ethidium bromide staining after electrophoretic separation (Fig. 5A). In the case of the DF-MITO-Porter, decreases in mtDNA-levels were observed (lanes 4, 5 in Fig. 5A (a)), whereas the effect of carriers with a low mitochondrial fusion activity on mtDNA-levels was negligible (lane 3 in Fig. 5A (a)). This result suggests that the mitochondrial delivery of DNase I by the DF-MITO-Porter resulted in a

measurable amount of mtDNA digestion. On the other hand, no decrease in nuclear DNA-levels was detected in any of the carriers (lanes 3-5 in Fig. 5A (b)).

We also quantified the levels of mtDNA and nuclear DNA within the cells based on the intensity of the band corresponding to the PCR product, and also performed a two-way ANOVA analysis (Fig. 5B). When the relative amount of DNA was compared among different lipid compositions, the levels of mtDNA were found to be significantly decreased by DF-MITO-Porter compared to carriers with a low mitochondrial fusogenic activity (**Significant difference ($p < 0.01$), closed bars in Fig. 5B). On the other hand, the nuclear DNA levels were not decreased in any of the carriers (No significant difference ($p < 0.01$), open bars in Fig. 5B). We next evaluated mtDNA levels against nuclear DNA levels for each lipid composition. In the case of a high mitochondrial fusogenic lipid composition, the mtDNA-levels were significantly lower than nuclear DNA levels (*Significant difference ($p < 0.005$), closed bar vs. open bar in Fig. 5B). Based on these results, it can be concluded that the mitochondrial specific fusion activity of the DF-MITO-Porter is involved in a pathway related to the selective digestion of mtDNA.

4. Discussion

In this study, we attempted to package a bioactive molecule via the use of a multifunctional envelope-type nano-device (MEND). The MEND consisted of a condensed pDNA core and a lipid envelope equipped with various functional devices that mimic envelope-type viruses [28, 29]. To date, we have been successful in efficiently packaging, not only pDNA, but also oligo DNAs, proteins and other substances into a MEND [30-33]. Various candidates for cargoes that can be used in conjunction with mitochondrial gene therapy and diagnosis are possible. For example, the delivery of wild-type mtDNA (circular DNA) to mitochondria in diseased cells would decrease the proportion of mutated mtDNA, thereby suppressing mitochondrial diseases [7, 12]. On the other hand, oligo DNA (linear DNA), as a therapeutic agent for muted mtDNA, was investigated, in order to repair mutated mtDNA and inhibit the replication of mutated mtDNA [34, 35]. Moreover, the use of a restriction enzyme (protein) would be expected to be useful and productive for the selective digestion of mutated mtDNA [36]. We conclude that the flexibility associated with the design of such a MEND will meet the requirements for drug delivery systems for mitochondrial gene therapy and diagnosis.

On the other hand, the MITO-Porter system delivers cargos into mitochondria via a membrane fusion mechanism [19]. We were also able to verify that the MITO-Porter delivered cargoes to the mitochondrial matrix, which pools mtDNA, using a ~~novel~~ fluorescent imaging method [20]. Therefore, large cargoes could be delivered to the mitochondrial matrix, provided that the cargoes can be encapsulated within the MITO-Porter. Accordingly, a combination of a MITO-Porter and a technique for packaging macromolecules in MEND preparations would likely permit the mitochondrial delivery of macromolecules such as mtDNA, oligo DNAs and proteins. In this experiment, we selected the DNase I protein as a model therapeutic agent for targeting the mitochondrial genome and attempted to package the bioactive protein in the DF-MITO-Porter.

We were interested in determining whether a conventional MITO-Porter (PA) and MITO-Porter (SM) would show different effects on mitochondrial activity (Fig. 3B), although both conventional MITO-Porters had high mitochondrial membrane fusogenic activities, as we previously reported [19]. The conventional MITO-Porter has a multi-lamellar structure composed of a single type of lipid envelope. Therefore, the conventional MITO-Porter must fuse with both endosomes and mitochondria, when this type of envelop is used. We previously determined the lipid composition including PA

[DOPE/PA/STR-R8 (7:2:1, molar ratio)] required for an optimal endosome-fusogenic composition. Taking this into consideration, it was presumed that a conventional MITO-Porter (PA) composed of DOPE/PA/STR-R8 (9:2:1, molar ratio) had a higher endosome-fusogenic activity than a conventional MITO-Porter (SM), resulting in an effective mitochondrial delivery. On the other hand, the DF-MITO-Porter resulted in significant decreases in mitochondrial activity independent of the lipid composition of the inner envelopes (Fig. 3A), suggesting that the outer envelope provides assistance in endosomal escape.

We showed that the mitochondrial delivery of DNase I by the DF-MITO-Porter drastically decreased mitochondrial activity (Fig. 3), and we also confirmed that the delivered DNase I selectively digested mtDNA (Fig. 5). These results were supported by the fact that the MITO-Porter has a high fusogenic activity for mitochondria, but that it failed to effectively fuse with the nucleus (Yamada et al, unpublished results). Based on these results, we were able to obtain information regarding the relationship between the mitochondrial activity and mtDNA digestion. It was presumed that mtDNA digestion would affect, not only mitochondrial gene expression, but also mitochondrial quality and quantity. One possibility is that a decrease in mitochondrial quality could lead to a reduction in mitochondrial activity. In a situation where mtDNA is digested, a

mitochondrion might need to use its energy for the production and repair of mtDNA, rather than for the maintenance of the mitochondrial respiratory chain. Another possibility is that a decrease in the numbers of mitochondria within one cell could have an influence on mitochondrial activity. A number of recent reports regarding mitophagy have appeared, reporting that mitochondria that are damaged are selectively eliminated [37]. Thus, damaged mitochondria containing digested mtDNA might be removed by mitophagy, thus decreasing the total mitochondrial activity in a cell.

5. Conclusion

In this study, we attempted to validate the possibility of mitochondrial genome targeting using a DF-MITO-Porter. The findings described here showed that the mitochondrial delivery of DNase I protein by the DF-MITO-Porter caused a substantial decrease in mitochondrial activity, suggesting that a multi-structured particle with a different lipid composition can be useful for mitochondrial delivery. In addition, we demonstrated that the mitochondrial delivery of DNase I by the DF-MITO-Porter resulted in the selective digestion of mtDNA. These results suggest that the DF-MITO-Porter holds promise as a delivery system targeted to mtDNA. Our ultimate goal is to develop mitochondrial gene therapy and diagnosis to the point where

therapeutic agents function on the mitochondrial genome. Future studies will involve attempts to improve the DF-MITO-Porter in terms of mitochondrial gene function with experts in the field of mitochondrial molecular biology. Studies directed toward this goal are currently in progress.

Acknowledgements

This work was supported, in part by, the Program for Promotion of Fundamental Studies in Health Sciences of the National Institute of Biomedical Innovation, Japan (NIBIO), a Grant-in-Aid for Young Scientists (A) and a Grant-in-Aid for Scientific Research (S) from the Ministry of Education, Culture, Sports, Science and Technology of Japanese Government (MEXT). We also thank Dr. Milton Feather for his helpful advice in writing the manuscript.

References

1. DiMauro S. Mitochondrial myopathies. Curr Opin Rheumatol. 2006;186:636-41.
2. Holt IJ, Harding AE, Morgan-Hughes JA. Deletions of muscle mitochondrial DNA in patients with mitochondrial myopathies. Nature. 1988;3316158:717-9.
3. Kagawa Y, Inoki Y, Endo H. Gene therapy by mitochondrial transfer. Adv Drug Deliv Rev. 2001;491-2:107-19.
4. Martin LJ. Mitochondriopathy in Parkinson disease and amyotrophic lateral sclerosis. J Neuropathol Exp Neurol. 2006;6512:1103-10.
5. Sarzi E, Brown MD, Lebon S, Chretien D, Munnich A, Rotig A, et al. A novel recurrent mitochondrial DNA mutation in ND3 gene is associated with isolated complex I deficiency causing Leigh syndrome and dystonia. Am J Med Genet A. 2007;1431:33-41.
6. Wallace DC. Mitochondrial diseases in man and mouse. Science. 1999;2835407:1482-8.
7. Wallace DC. The mitochondrial genome in human adaptive radiation and disease: on the road to therapeutics and performance enhancement. Gene. 2005;354:169-80.
8. Goto Y, Nonaka I, Horai S. A mutation in the tRNA(Leu)(UUR) gene associated with the MELAS subgroup of mitochondrial encephalomyopathies. Nature. 1990;3486302:651-3.
9. Shoffner JM, Lott MT, Lezza AM, Seibel P, Ballinger SW, Wallace DC. Myoclonic epilepsy and ragged-red fiber disease (MERRF) is associated with a mitochondrial DNA tRNA(Lys) mutation. Cell. 1990;616:931-7.
10. Shanske S, Moraes CT, Lombes A, Miranda AF, Bonilla E, Lewis P, et al. Widespread tissue distribution of mitochondrial DNA deletions in Kearns-Sayre syndrome. Neurology. 1990;401:24-8.
11. Mukhopadhyay A, Weiner H. Delivery of drugs and macromolecules to mitochondria. Adv Drug Deliv Rev. 2007;598:729-38.
12. Yamada Y, Harashima H. Mitochondrial drug delivery systems for macromolecule and their therapeutic application to mitochondrial diseases. Adv Drug Deliv Rev. 2008;6013-14:1439-62.
13. Zhang E, Zhang C, Su Y, Cheng T, Shi C. Newly developed strategies for multifunctional mitochondria-targeted agents in cancer therapy. Drug Discov Today. 2011;163-4:140-6.

14. Mukherjee S, Mahata B, Mahato B, Adhya S. Targeted mRNA degradation by complex-mediated delivery of antisense RNAs to intracellular human mitochondria. Hum Mol Genet. 2008;179:1292-8.
15. Mahata B, Mukherjee S, Mishra S, Bandyopadhyay A, Adhya S. Functional delivery of a cytosolic tRNA into mutant mitochondria of human cells. Science. 2006;3145798:471-4.
16. Weissig V, D'Souza GG, Torchilin VP. DQAsome/DNA complexes release DNA upon contact with isolated mouse liver mitochondria. J Control Release. 2001;753:401-8.
17. D'Souza GG, Rammohan R, Cheng SM, Torchilin VP, Weissig V. DQAsome-mediated delivery of plasmid DNA toward mitochondria in living cells. J Control Release. 2003;921-2:189-97.
18. D'Souza GG, Boddapati SV, Weissig V. Mitochondrial leader sequence--plasmid DNA conjugates delivered into mammalian cells by DQAsomes co-localize with mitochondria. Mitochondrion. 2005;55:352-8.
19. Yamada Y, Akita H, Kamiya H, Kogure K, Yamamoto T, Shinohara Y, et al. MITO-Porter: A liposome-based carrier system for delivery of macromolecules into mitochondria via membrane fusion. Biochim Biophys Acta. 2008;17782:423-32.
20. Yasuzaki Y, Yamada Y, Harashima H. Mitochondrial matrix delivery using MITO-Porter, a liposome-based carrier that specifies fusion with mitochondrial membranes. Biochem Biophys Res Commun. 2010;3972:181-6.
21. Yamada Y, Furukawa R, Yasuzaki Y, Harashima H. Dual Function MITO-Porter, a Nano Carrier Integrating Both Efficient Cytoplasmic Delivery and Mitochondrial Macromolecule Delivery. Mol Ther. 2011.
22. Futaki S, Suzuki T, Ohashi W, Yagami T, Tanaka S, Ueda K, et al. Arginine-rich peptides. An abundant source of membrane-permeable peptides having potential as carriers for intracellular protein delivery. J Biol Chem. 2001;2768:5836-40.
23. Nakase I, Niwa M, Takeuchi T, Sonomura K, Kawabata N, Koike Y, et al. Cellular uptake of arginine-rich peptides: roles for macropinocytosis and actin rearrangement. Mol Ther. 2004;106:1011-22.
24. Asoh S, Ohsawa I, Mori T, Katsura K, Hiraide T, Katayama Y, et al. Protection against ischemic brain injury by protein therapeutics. Proc Natl Acad Sci U S A. 2002;9926:17107-12.
25. Del Gaizo V, Payne RM. A novel TAT-mitochondrial signal sequence fusion protein is processed, stays in mitochondria, and crosses the placenta. Mol Ther. 2003;76:720-30.

26. Futaki S, Ohashi W, Suzuki T, Niwa M, Tanaka S, Ueda K, et al. Stearylated arginine-rich peptides: a new class of transfection systems. Bioconjug Chem. 2001;126:1005-11.
27. El-Sayed A, Khalil IA, Kogure K, Futaki S, Harashima H. Octaarginine- and octalysine-modified nanoparticles have different modes of endosomal escape. J Biol Chem. 2008;28334:23450-61.
28. Kogure K, Akita H, Yamada Y, Harashima H. Multifunctional envelope-type nano device (MEND) as a non-viral gene delivery system. Adv Drug Deliv Rev. 2008;604-5:559-71.
29. Kogure K, Moriguchi R, Sasaki K, Ueno M, Futaki S, Harashima H. Development of a non-viral multifunctional envelope-type nano device by a novel lipid film hydration method. J Control Release. 2004;982:317-23.
30. Suzuki R, Yamada Y, Harashima H. Efficient Cytoplasmic Protein Delivery by Means of a Multifunctional Envelope-type Nano Device. Biol Pharm Bull. 2007;304:758-62.
31. Homhuan A, Kogure K, Akaza H, Futaki S, Naka T, Fujita Y, et al. New packaging method of mycobacterial cell wall using octaarginine-modified liposomes: enhanced uptake by and immunostimulatory activity of dendritic cells. J Control Release. 2007;1201-2:60-9.
32. Nakamura Y, Kogure K, Yamada Y, Futaki S, Harashima H. Significant and prolonged antisense effect of a multifunctional envelope-type nano device encapsulating antisense oligodeoxynucleotide. J Pharm Pharmacol. 2006;584:431-7.
33. Yamada Y, Kogure K, Nakamura Y, Inoue K, Akita H, Nagatsugi F, et al. Development of efficient packaging method of oligodeoxynucleotides by a condensed nano particle in lipid envelope structure. Biol Pharm Bull. 2005;2810:1939-42.
34. Chen Z, Felsheim R, Wong P, Augustin LB, Metz R, Kren BT, et al. Mitochondria isolated from liver contain the essential factors required for RNA/DNA oligonucleotide-targeted gene repair. Biochem Biophys Res Commun. 2001;2852:188-94.
35. Taylor RW, Chinnery PF, Turnbull DM, Lightowlers RN. Selective inhibition of mutant human mitochondrial DNA replication in vitro by peptide nucleic acids. Nat Genet. 1997;152:212-5.
36. Tanaka M, Borgeld HJ, Zhang J, Muramatsu S, Gong JS, Yoneda M, et al. Gene therapy for mitochondrial disease by delivering restriction endonuclease SmaI into mitochondria. J Biomed Sci. 2002;96 Pt 1:534-41.
37. Youle RJ, Narendra DP. Mechanisms of mitophagy. Nat Rev Mol Cell Biol.

2011;121:9-14.

Figure legends

Figure 1. Schematic image of mitochondrial delivery of bioactive molecules for targeting the mitochondrial genome using DF-MITO-Porter.

This figure shows the strategy behind the mitochondrial delivery of DNase I protein via a series of membrane fusions using a Dual Function (DF)-MITO-Porter, aimed at the mitochondrial genome (mtDNA). Complexed particles of DNase I proteins are coated with a mitochondria-fusogenic lipid envelope (inner) and an endosome-fusogenic lipid envelope (outer). Octaarginine (R8) functions as a cell-uptake device in the outer envelope and as a mitochondrial targeting device in the inner envelope. The DF-MITO-Porter is surface-modified with a high density of R8, which can be efficiently internalized by cells (1st step). Once inside the cell, the carrier escapes from the endosome into the cytosol via membrane fusion, a process that is mediated by the outer endosome-fusogenic lipid membranes (2nd step). The carrier then binds to mitochondria via electrostatic interactions with R8 (3rd step) and fuses with the mitochondrial membrane to deliver the cargos to mitochondria (4th step). Finally, DNase I proteins digest mtDNA, resulting in the decrease of mitochondrial activity (5th step).

Figure 2. Intracellular observation of DF-MITO-Porter using confocal laser scanning microscopy

DF-MITO-Porter (A) and conventional MITO-Porter (B) encapsulating DNase I protein labeled with Alexa 488 as a tracer were incubated with HeLa cells. Mitochondria were stained with Mitofluor Red 589 prior to

intracellular observation. DNase I proteins (green) are seen to be co-localized with mitochondria (red), observed as a yellow signal in the merged images. Scale bars, 10 μm.

Figure 3. Mitochondrial delivery of DNase I using DF-MITO-Porter and conventional MITO-Porter. (**A**) DNase I (0.5 μg) encapsulated in DF-MITO-Porter (SM), DF-MITO-Porter (PA) or control carrier with low mitochondrial fusion activity were incubated with HeLa cells. Mitochondrial activity was then evaluated by measuring mitochondrial dehydrogenase activity. (**B**) Mitochondrial activities were also evaluated, when DNase I (6.25 μg) encapsulated in conventional MITO-Porter and control carrier with low mitochondrial fusion activity were used. Data are represented as the mean ± S.D. (n = 3-4). **Significant differences between control carrier (EPC/CHEMS/STR-R8) and other carriers ($p < 0.01$ by one-way ANOVA, followed by Bonferroni correction).

Figure 4. Comparison of mitochondrial activity after DNase I delivery between DF-MITO-Porter and conventional MITO-Porter. The closed and open circles represent the values corresponding to the mitochondrial activity (%), when DF-MITO-Porter (PA) and conventional MITO-Porter (PA) were used. Data are represented as the mean ± S.D. (n = 3-4). We also calculated effective dose 50 (ED_{50}) of each carriers.

Figure 5. Evaluation for the levels of mtDNA and nuclear DNA after the mitochondrial delivery of DNase I. DNase I proteins encapsulated in the DF-MITO-Porter (SM), the DF-MITO-Porter (PA) or the control carrier

with low mitochondrial fusion activity were incubated with HeLa cells. Cellular DNA were collected and then subjected to the PCR. The PCR products were detected by ethidium bromide staining after separation by electrophoresis (**A**). PCR assays for the ND6 and β-Actin genes detection were performed in order to detect both mtDNA (**a**) and nuclear DNA (**b**), respectively. Lane 1, 100 bp DNA Ladder; lane 2, Non-treatment; lane 3, control carrier with low mitochondrial fusion activity [EPC/CHEMS/STR-R8]; lane 4, DF-MITO-Porter (SM); lane 5, DF-MITO-Porter (PA). ND6, mitochondrial NADH dehydrogenase 6. We also quantified the levels of mtDNA and nuclear DNA within the cells based on the intensity of the bands corresponding to the PCR product, and then performed two-way ANOVA analysis (**B**). Data are represented as the mean ± S.D. (n = 3). **Significant differences between control carrier (EPC/CHEMS/STR-R8) and other carriers among different lipid compositions ($p < 0.01$ by two-way ANOVA, followed by Bonferroni correction). *Significant differences between mtDNA levels and nuclear DNA levels for each lipid compositions ($p < 0.005$ by two-way ANOVA, followed by Bonferroni correction).

Fig. 1

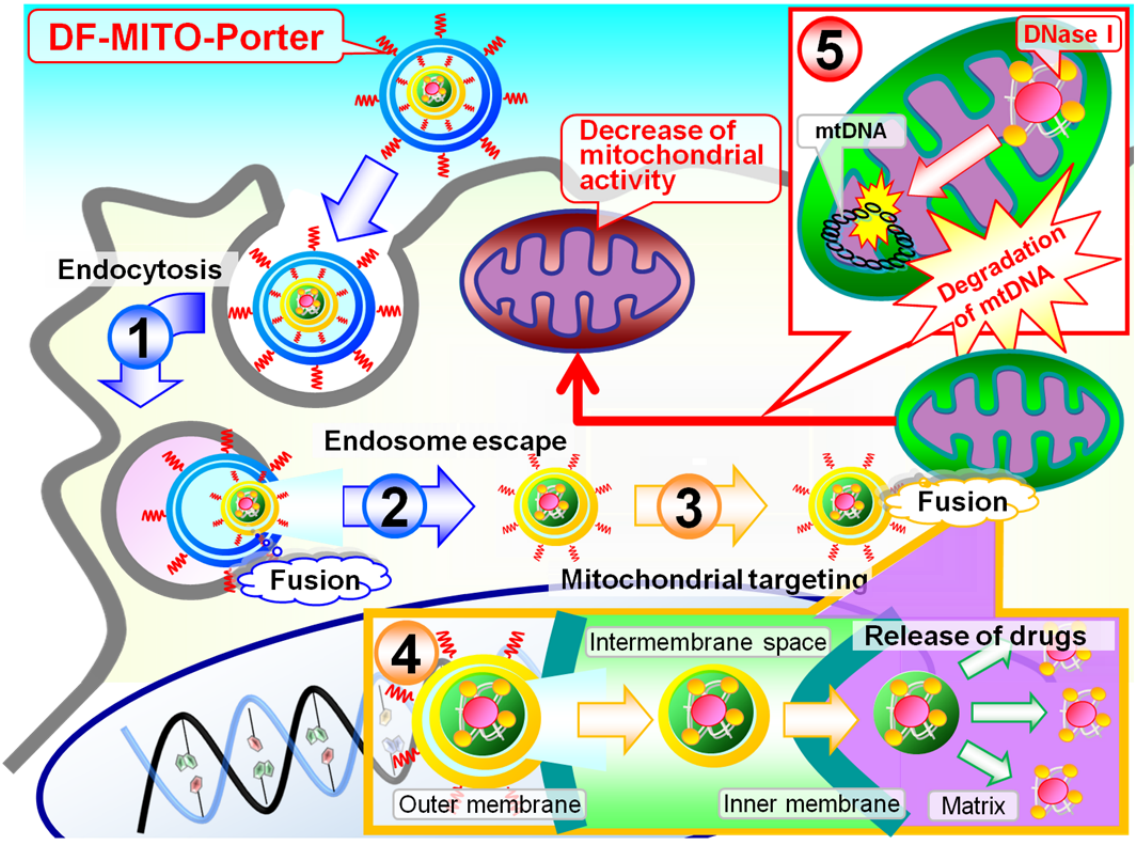
DF-MITO-Porter
Endocytosis
1
Endosome escape
2
Fusion
3
Fusion
Mitochondrial targeting
Decrease of mitochondrial activity
5
DNase I
mtDNA
Degradation of mtDNA
4
Intermembrane space
Release of drugs
Outer membrane
Inner membrane
Matrix

Fig. 2

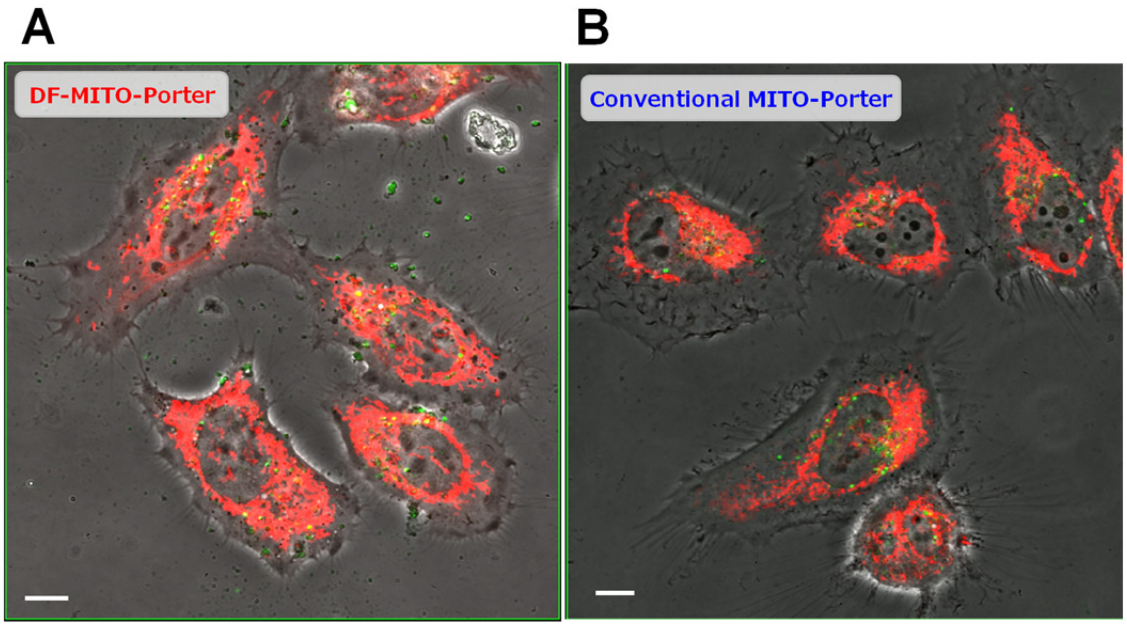

Fig. 3

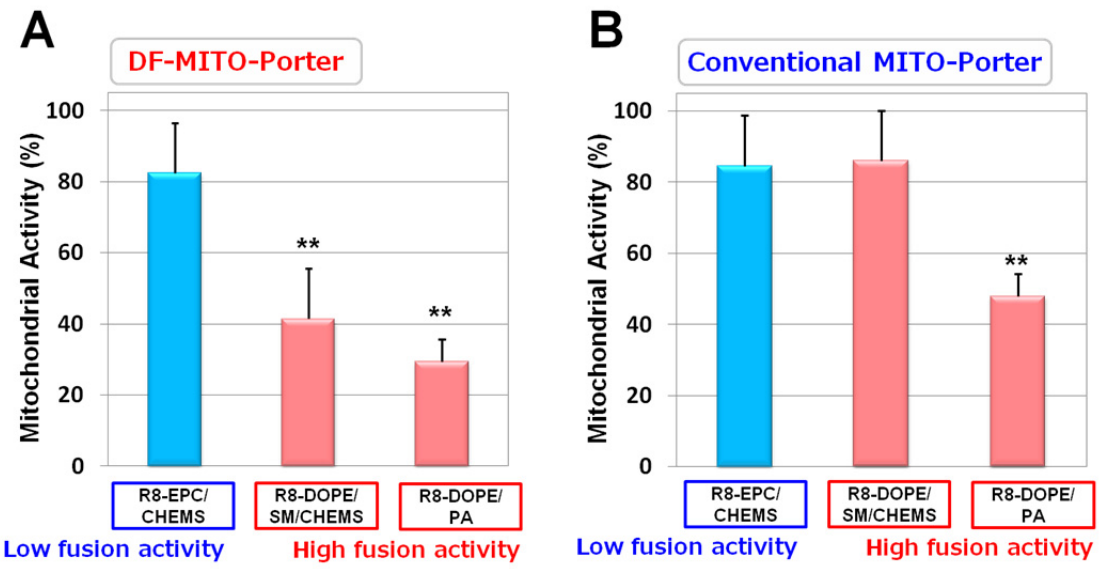
A
DF-MITO-Porter
Mitochondrial Activity (%)
100
80
60
40
20
0
**
**
R8-EPC/ CHEMS
R8-DOPE/ SM/CHEMS
R8-DOPE/ PA
Low fusion activity
High fusion activity
B
Conventional MITO-Porter
Mitochondrial Activity (%)
100
80
60
40
20
0
**
R8-EPC/ CHEMS
R8-DOPE/ SM/CHEMS
R8-DOPE/ PA
Low fusion activity
High fusion activity

Fig. 4

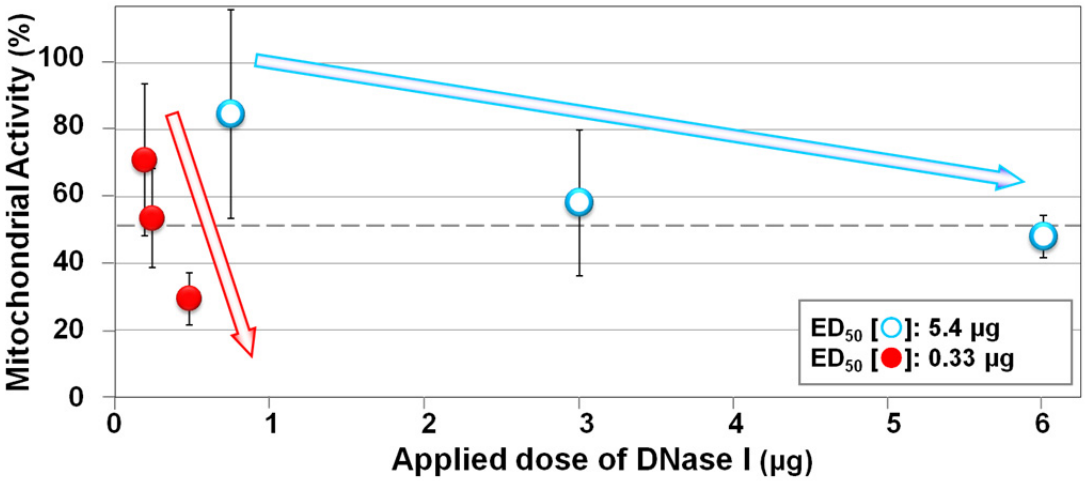
Mitochondrial Activity (%)
100
80
60
40
20
0
0
1
2
3
4
5
6
Applied dose of DNase I (µg)
ED50 [○]: 5.4 µg
ED50 [●]: 0.33 µg

Fig. 5

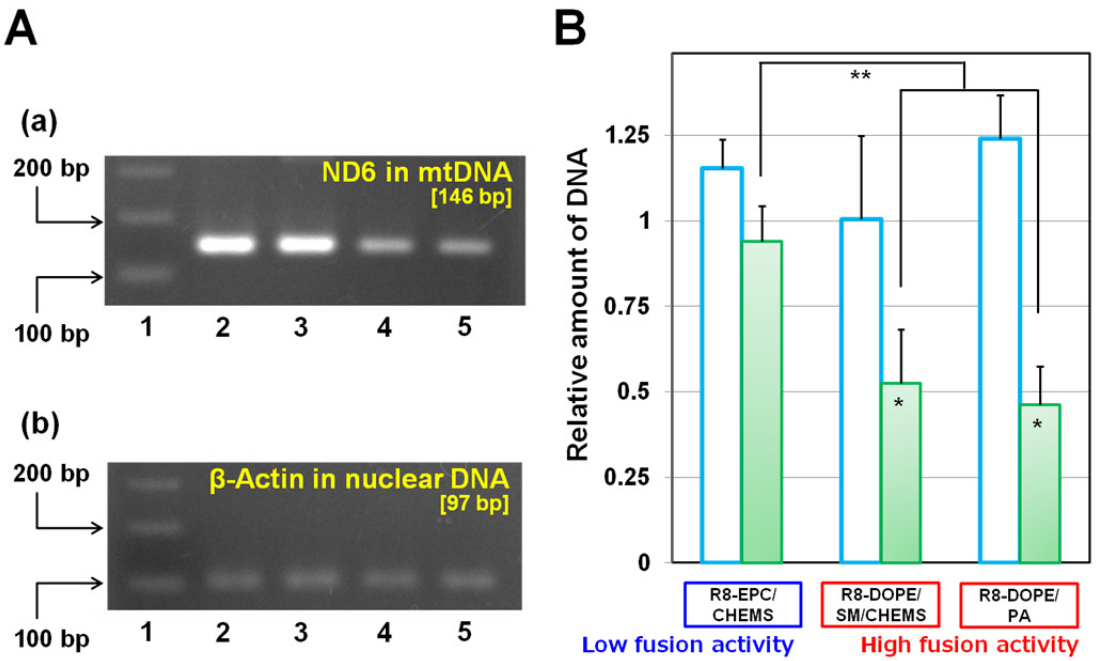
A
(a)
200 bp
100 bp
ND6 in mtDNA
[146 bp]
1 2 3 4 5
(b)
200 bp
100 bp
β-Actin in nuclear DNA
[97 bp]
1 2 3 4 5
B
Relative amount of DNA
1.25
1
0.75
0.5
0.25
0
**
*
*
R8-EPC/ CHEMS
R8-DOPE/ SM/CHEMS
R8-DOPE/ PA
Low fusion activity
High fusion activity

Supplementary data

Delivery of bioactive molecules to the mitochondrial genome using a membrane-fusing, liposome-based carrier, DF-MITO-Porter

Yuma Yamada[a] and Hideyoshi Harashima[a]*

[a] Laboratory for molecular design of pharmaceutics, Faculty of Pharmaceutical Sciences, Hokkaido University, Kita-12, Nishi-6, Kita-ku, Sapporo 060-0812, Japan

*Corresponding author: Laboratory for molecular design of pharmaceutics, Faculty of Pharmaceutical Sciences, Hokkaido University, Kita-12, Nishi-6, Kita-ku, Sapporo 060-0812, Japan

Tel: +81-11-706-3919 Fax: +81-11-706-4879

E-mail: harasima@pharm.hokudai.ac.jp

1. Materials and Methods

1.1. SUV preparation

Small unilamellar vesicles (SUVs) with various lipid compositions, as shown in Table S1, were prepared by the following procedure. A 1.5 mL aliquot of 10 mM HEPES buffer (pH 7.4) was applied to 825 nmol of a dried lipid film formed on the bottom of a glass tube. After incubation for 10 min, the suspensions were sonicated using a bath-type sonicator (85 W, Aiwa Co., Tokyo, Japan) for 15 sec. The resulting suspensions were then sonicated using a probe-type sonicator (SONIFIER MODEL 250 D, BRANSON, Danbury, CT, USA) for 10 min on ice to form SUV.

1.2.Construction of the conventional MITO-Porter encapsulating DNase I

The conventional MITO-Porter encapsulating DNase I was constructed by the following three steps. First, 1 mg/ml of DNase I protein dissolved in 10 mM HEPES buffer (HB, pH 7.4) was mixed with a stearyl octaarginine (STR-R8) solution, at a C/P molar ratio of 10, to form complexed protein particles by gently pipetting, followed by incubation for 15 min at 25ºC. The suspension of complexed protein particles was diluted with HB to 0.125 mg/mL of DNase I protein. Then, 0.25 ml of the resulting suspension was added to the lipid film, formed by the evaporation of a chloroform

solution of 137.5 nmol lipids on the bottom of a glass tube, followed by incubation for 15 min to hydrate the lipids. The glass tube was sonicated to coat the complexed protein particle with lipids in a bath-type sonicator (85 W; Aiwa Co., Tokyo, Japan) for 15 sec. To attach octaarginine (R8) to the surface of the carrier, a solution of STR-R8 (10 mol% lipids) was added to the resulting suspensions. The envelope of the conventional MITO-Porters had a mitochondria-fusogenic composition [DOPE/SM/CHEMS/STR-R8 (9:2:1:1, molar ratio) or DOPE/PA/STR-R8 (9:2:1, molar ratio)], while a non-mitochondrial fusogenic composition [EPC/CHEMS/STR-R8 (9:2:1, molar ratio)] was used in the control carrier.

2. Supplementary Figure

Figure S1. Schematic diagram of the preparation of the DF-MITO-Porter.

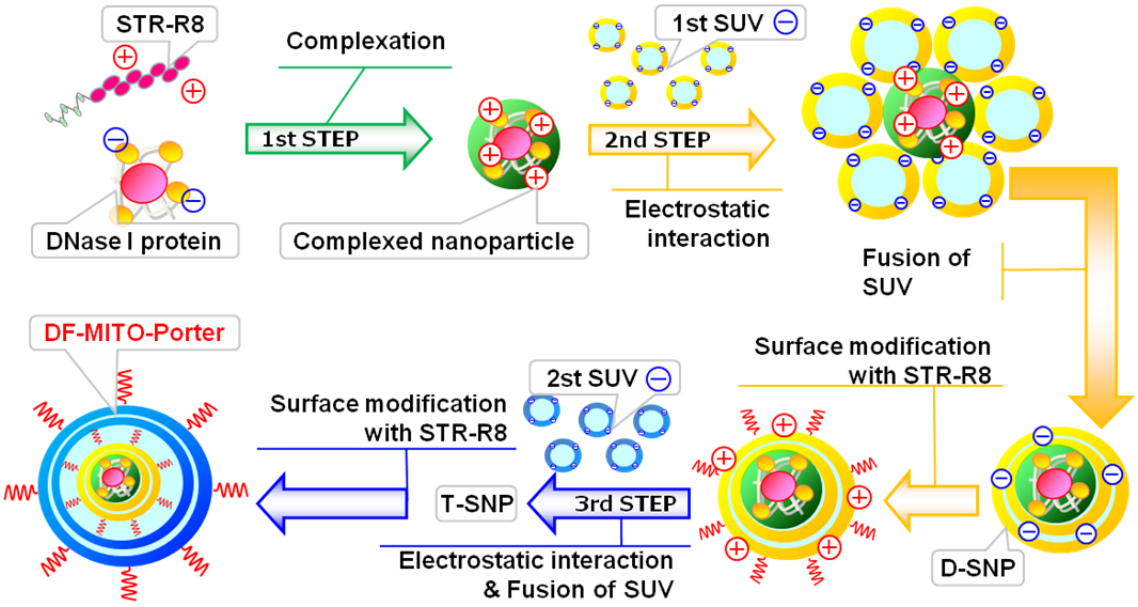

The construction of the DF-MITO-Porter encapsulating DNase I requires the following three steps: (1) the construction of nano particles containing DNase I; (2) coating the nanoparticles with a mitochondria-fusogenic envelope; (3) further coating the endosome-fusogenic envelope in a step-wise manner with two-different types of lipid layers, based on our previous report regarding gene packaging [1]. The complexed nanoparticle of DNase I protein was first prepared with stearyl octaarginine (STR-R8) [2] that would be suitable for the complexation of proteins [3]. A di-lamellar structured nanoparticle (D-SNP) was then prepared through membrane fusion of neighboring small unilamellar vesicle (SUV)s, triggered by the assembly of negatively charged SUVs around the positively charged complexed nanoparticle of DNase I protein. The

surface of the resulting particles is then modified with STR-R8 to reverse the surface charge. Octaarginine (R8)-modified D-SNP was next coated with the second envelope, again through the fusion of negatively charged SUV to produce tetra-lamellar structured nanoparticle (T-SNP). Finally, the STR-R8 solution was added to the suspension of T-SNP to modify the outer envelope with R8 and construct the DF-MITO-Porter.

3. Supplementary Table

Table S1. Lipid composition and property of SUVs.

Inner or Outer envelopes	Lipid compositions	Diameter (nm)	ζ potential (mV)	Property
Inner envelope (1st SUV)	DOPE/SM/CHEMS (9/2/1, molar ratio)	61 ± 4	-36 ± 7	Mitochondria-fusogenic composition, when the SUV-surface is modified with 10 mol% of STR-R8.
	DOPE/PA (9/2, molar ratio)	59 ± 2	-66 ± 1	
	EPC/CHEMS (9/2, molar ratio)	46 ± 2	-29 ± 16	Non-fusogenic composition.
Outer envelope (2nd SUV)	DOPE/PA (7/2, molar ratio)	59 ± 2	-53 ± 5	Endosome-fusogenic composition, when the SUV-surface is modified with 10 mol% of STR-R8.

Lipid composition and properties of the SUVs are summarized in Table S1. We previously reported on these characteristics of SUVs for the preparation of DF-MITO-Porter [4]. DOPE, 1,2-dioleoyl-sn-glycero-3-phosphatidyl ethanolamine; PA, phosphatidic acid; CHEMS, cholesteryl hemisuccinate (5-cholesten-3-ol 3-hemisuccinate); SM, sphingomyelin; EPC, egg yolk phosphatidyl choline. Data are represented as the mean ± S.D. (n=3-6).

Table S2. Primers used in the PCR to evaluate the levels of mtDNA and nuclear DNA.

Primers	Nucleotide sequence	Location of target genome	Annealing site in genome (PCR products size)
ND6 (+)	5' ATAGGATCCTCCCGAATCAA 3'	Mitochondria	106-251 in ND6 region of mitochondrial genome (146 bp)
ND6 (-)	5' GTTTTAGTGGGGTTAGCGAT 3'		
β-Actin (+)	5' CCCAAAGTTCACAATGTGG 3'	Nucleus	1402-1498 in β-Actin region of nuclear genome (97 bp)
β-Actin (-)	5' AAGGGACTTCCTGTAACAAC 3'		

PCR assays to detect the ND6 and β-Actin genes were performed in order to detect mtDNA and nuclear DNA of HeLa cell lysates, respectively. ND6, mitochondrial NADH dehydrogenase 6.

Table S3. Characteristics of the DF-MITO-Porter and conventional MITO-Porter.

Lipid compositions (Inner envelope)	Dual Function MITO-Porter		Conventional MITO-Porter	
	Diameter (nm)	ζ potential (mV)	Diameter (nm)	ζ Potential (mV)
DOPE/SM/CHEMS/STR-R8 (9:2:1:1)	152 ± 9	35 ± 8	215 ± 42	44 ± 6
DOPE/PA/STR-R8 (9:2:1)	157 ± 12	34 ± 10	235 ± 19	37 ± 7
EPC/CHEMS/STR-R8 (9:2:1)	112 ± 6	31 ± 2	123 ± 8	39 ± 4

Diameters and ζ-potentials of the DF-MITO-Porter and conventional MITO-Porter are summarized in Table S3. We previously reported these characteristics [4]. Data are represented as the mean ± S.D. (n = 3-4). DOPE, 1,2-dioleoyl-sn-glycero-3-phosphatidyl ethanolamine; PA, phosphatidic acid; CHEMS, cholesteryl hemisuccinate (5-cholesten-3-ol 3-hemisuccinate); SM, sphingomyelin; EPC, egg yolk phosphatidyl choline.

References

[1] H. Akita, A. Kudo, A. Minoura, M. Yamaguti, I.A. Khalil, R. Moriguchi, T. Masuda, R. Danev, K. Nagayama, K. Kogure, H. Harashima, Multi-layered nanoparticles for penetrating the endosome and nuclear membrane via a step-wise membrane fusion process, Biomaterials 30 (2009) 2940-2949.

[2] S. Futaki, W. Ohashi, T. Suzuki, M. Niwa, S. Tanaka, K. Ueda, H. Harashima, Y. Sugiura, Stearylated arginine-rich peptides: a new class of transfection systems, Bioconjug Chem 12 (2001) 1005-1011.

[3] R. Suzuki, Y. Yamada, H. Harashima, Efficient cytoplasmic protein delivery by means of a multifunctional envelope-type nano device, Biol Pharm Bull 30 (2007) 758-762.

[4] Y. Yamada, R. Furukawa, Y. Yasuzaki, H. Harashima, Dual function MITO-Porter, a nano carrier integrating both efficient cytoplasmic delivery and mitochondrial macromolecule delivery, Mol Ther (2011).